Synthesis, crystal structure and luminescence properties of eight new lanthanide carboxyphosphonates with a 3D framework structure†‡

Na Zhang, Zhengang Sun,* Yanyu Zhu, Jing Zhang, Lei Liu, Cuiying Huang, Xin Lu, Weinan Wang and Fei Tong

Received (in Gainesville, FL, USA) 5th September 2009, Accepted 19th May 2010
DOI: 10.1039/b9nj00456d

By using the carboxyphosphonic acid as the ligand, eight new three-dimensional (3D) lanthanide carboxyphosphonates, namely $Ln[L(H_2O)_2]\cdot 2H_2O$ (Ln = Ce (**1**), Pr (**2**), Nd (**3**), Sm (**4**), Eu (**5**), Gd (**6**), Y (**7**), Tb (**8**); H_3L = $H_2O_3PCH_2$–NC_5H_9–COOH) have been synthesized under hydrothermal conditions and structurally characterized by X-ray single-crystal diffraction, X-ray powder diffraction, infrared spectroscopy, elemental analysis and thermogravimetric analysis. The eight isomorphous compounds feature a 3D framework structure. In these compounds, the inorganic chains based on LnO_8 and CPO_3 polyhedra are interconnected through carboxyphosphonate ligands to form a 3D framework structure with a channel system. The result of connections in this manner is the formation of 40- and 24-atom rings that run in the *a*- and *b*-axis directions. The luminescence properties of compounds **5** and **8** have also been studied.

Introduction

Metal phosphonates have received extensive research attention in recent years due to the possibility to form interesting structures with potential applications in the areas of catalysis, ion exchange, proton conductivity, intercalation chemistry, photochemistry and materials chemistry.[1–5] Many efforts have been devoted to the exploration of metal phosphonate materials with new structural types, especially open-framework structures.[6–11] It is well-known that organic ligands play a crucial role in the design and construction of desirable frameworks. The strategy of attaching additional functional groups such as amine, hydroxyl, and carboxylate groups to the phosphonic acid has been proved to be very effective in building open-framework and microporous structures.[12–16] Among these functional groups, the carboxyl has been used widely because of its coordination ability.

The use of carboxyphosphonic acids in the synthesis of three-dimensional (3D) framework structures has attracted much interest over the last few years. A series of metal carboxyphosphonates with a framework structure (using $HOOC–CH_2–PO_3H_2$ and $HOOC–CH_2CH_2–PO_3H_2$ as ligands) have been isolated, mainly by the Cheetham, Bujoli, and Sevov groups.[17–19] Results from our laboratory and other groups indicate that carboxyphosphonic acids, such as $HOOC–RNHCH_2PO_3H_2$ and $HOOC–RN–(CH_2PO_3H_2)_2$ (where R is an organic group), are also good candidates for the synthesis of metal phosphonates with open-framework structures, in which the organic part plays a controllable spacer role and the –COOH and $–PO_3$ groups chelate with metal ions to form novel structure types.[20–22] An investigation on the synthesis of metal phosphonate hybrids based on $H_2O_3PCH_2$–NC_5H_9–COOH has recently led to the first microporous three-dimensional lanthanide carboxyphosphonates, $Pr_4(H_2O)_7[O_2C–C_5H_{10}N–CH_2–PO_3]_4(H_2O)_5$.[23] By using $H_2O_3PCH_2$–NC_5H_9–COOH (H_3L) as the building block, a novel 3D cadmium carboxyphosphonate containing left-hand helical chain, $Cd_3Cl_2[(O_3PCH_2–N(H)C_5H_9–COO)_2(H_2O)_2]\cdot 4H_2O$, has also been isolated by our group.[24]

In recent years, our interest in metal phosphonate chemistry has been extended to the lanthanides, and a series of lanthanide oxalatophosphonates with a 3D framework structure have been obtained in our laboratory.[25] Lanthanide phosphonates normally have low solubility in water and other organic solvents; hence, it is difficult to obtain single crystals suitable for X-ray structural analysis. To improve the solubility and crystallinity of lanthanide phosphonates, additional functional groups such as amine, hydroxyl, and carboxylate groups have been attached to the phosphonic acid ligand.[26–28] As an extension of our previous work on lanthanide phosphonates, in this work we selected carboxyphosphonic acid, $H_2O_3PCH_2$–NC_5H_9–COOH (H_3L) as the phosphonate ligand. Hydrothermal reactions of H_3L with lanthanide(III) chlorides resulted in eight new lanthanide carboxyphosphonates with a 3D framework structure, namely, $Ln[L(H_2O)_2]\cdot 2H_2O$ (Ln = Ce (**1**), Pr (**2**), Nd (**3**), Sm (**4**), Eu (**5**), Gd (**6**), Y (**7**), Tb (**8**)). Herein we report their syntheses, crystal structures and thermal stabilities. The luminescence properties of compounds **5** and **8** have also been studied.

Institute of Chemistry for Functionalized Material, School of Chemistry and Chemical Engineering, Liaoning Normal University, Dalian 116029, P. R. China. E-mail: szg188@163.com; Fax: +8641182156858

† Electronic supplementary information (ESI) available: Additional experimental information. CCDC reference numbers 705906 (**1**), 705907 (**2**), 705908 (**3**), 705909 (**4**), 745823 (**5**), 705910 (**6**) and 705911 (**7**). For ESI and crystallographic data in CIF or other electronic format see DOI: 10.1039/b9nj00456d

‡ This article is part of a themed issue on Coordination polymers: structure and function.

Results and discussion

Synthesis

By using the carboxyphosphonic acid as the ligand, eight new lanthanide(III) carboxyphosphonates with a 3D framework structures have been synthesized under hydrothermal conditions. The compounds **1–8** were obtained as pure phases by adjusting the synthetic conditions. Results indicate that the molar ratio of starting materials and the pH value play an important role during the reaction. It was found that pure phases of compounds **1–8** can be obtained with good yields when the molar ratio of $LnCl_3{\cdot}6H_2O$ and H_3L is 1 : 1. NaOH was added into the reaction system directly in the form of a solid, to adjust the pH of the reaction mixture. The initial and final pH values of the resultant solution are about 3.5 and 6, respectively. In addition, the reaction temperature was very important for the formation of suitable single crystals for X-ray diffraction. Compounds **1–4**, **6** and **7** were obtained at 140 °C under hydrothermal conditions. However, compounds **5** and **8** were obtained at 120 °C and 80 °C, respectively. The powder XRD patterns of compounds **1–8** and the simulated XRD patterns of compound **1** are shown in supplementary material (Fig. S1†). The diffraction peaks on the patterns correspond well in position, confirming that these eight compounds are isomorphous and phase-pure. Despite all our efforts to grow single crystals of compound **8**, we were not successful in obtaining a good sample for X-ray diffraction study. However, X-ray powder diffraction analysis indicates that compounds **1–8** are isomorphous. The differences in reflection intensity are probably due to the preferred orientation in the powder samples.

Description of the crystal structures

Compounds **1–8** are isomorphous and feature a 3D framework structure; hence only the structure of **3** will be discussed in detail as a representative example. The ORTEP diagram for compound **3** is shown in Fig. 1. Crystallographic data and structural refinements for compounds **1–7** are summarized in Table 1.

As shown in Fig. 1, the asymmetric unit of **3** contains one crystallographically unique neodymium(III) ion, one L^{3-} anion, and two coordinated water molecules. The Nd(III) center is eight-coordinated by two phosphonate oxygen atoms (O1, O2)

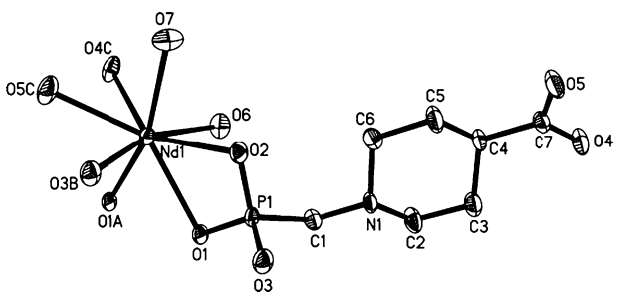

Fig. 1 ORTEP representation of a selected unit of compound **3**. The thermal ellipsoids are drawn at the 50% probability level. All H atoms and solvate water molecules are omitted for clarity. Symmetry codes: A: $-x+1, -y+2, -z+2$; B: $-x, -y+2, -z+2$; C: $x+1, -y+\frac{3}{2}, z+\frac{1}{2}$.

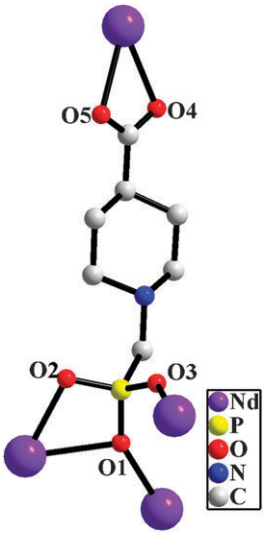

Fig. 2 Coordination fashions of carboxyphosphonate ligands in compound **3**.

from one L^{3-} anion, two phosphonate oxygen atoms (O1A, O3B) from another two L^{3-} anions, two carboxyl oxygen atoms (O4C, O5C) from other L^{3-} anion, and two oxygen atoms (O11, O12) from two coordinated water molecules. The Nd–O distances are in the range 2.343(4)–2.581(4) Å (Table S1†), which are comparable to those reported for other Nd(III) phosphonates.[29] Each L^{3-} acts as a μ_4-bridge to link four Nd(III) atoms through all its phosphonate oxygen atoms and carboxyl oxygen atoms (Fig. 2). It is interesting to note that the coordinating mode of three phosphonate oxygen atoms is different. The phosphonate oxygen atom (O3) of the H_3L ligand bridges one Nd atom in monodentate fashion, the phosphonate oxygen atom (O1) connects two Nd atoms, and two phosphonate oxygen atoms (O1, O2) chelate one Nd atom. Moreover, the carboxylate group adopts a μ_1–η^1:η^1-bridging coordination mode to ligate one Nd(III) atom.

In compound **3**, two NdO_8 polyhedra are interconnected into a dimer through edge-sharing. Each edge-sharing Nd_2O_{14} dimer is linked to each other through CPO_3 tetrahedra, and thereby form inorganic chain. As shown in Fig. 3a, such inorganic chains are interconnected through carboxyphosphonate ligands to form a 3D framework structure with a channel system. The result of connections in this manner is the formation of 40-atom rings along the *a*-axis (Fig. 3b). The channel is assembled with 40 atoms [21.6 Å (Nd1–Nd1) × 13.4 Å (P1–P1)], which is composed of four Nd, four P, four N, eight O and twenty C atoms, and the lattice water molecules are located in the channels. Viewed down the *b*-axis, the framework of compound **3** also displays a channel system (Fig. 4a). The channel is formed by 24-atom rings [11.5 Å (Nd1–P1) × 5.0 Å (N1–N1)] with the sequences Nd–O–P–O–Nd–O–C–C–C–C–N–C–P–O–Nd–O–P–C–N–C–C–C–C–O (Fig. 4b). The connection of alternating inorganic chains and carboxyphosphonate ligands results in an infinite 3D six-connected net. For a clearer representation, the Nd_2O_{14} units are represented by spherical SBUs, and carboxyphosphonate ligands are represented by sticks (Fig. 5). Interestingly, the framework can be described as a distorted primitive cubic

Table 1 Crystal data and structure refinements for compounds **1–7**

	Ce[$L(H_2O)_2$]·$2H_2O$	Pr[$L(H_2O)_2$]·$2H_2O$	Nd[$L(H_2O)_2$]·$2H_2O$	Sm[$L(H_2O)_2$]·$2H_2O$	Eu[$L(H_2O)_2$]·$2H_2O$	Gd[$L(H_2O)_2$]·$2H_2O$	Y[$L(H_2O)_2$]·$2H_2O$
Formula[a]	$C_7H_{19}NO_9PCe$	$C_7H_{19}NO_9PPr$	$C_7H_{19}NO_9PNd$	$C_7H_{19}NO_9PSm$	$C_7H_{19}NO_9PEu$	$C_7H_{19}NO_9PGd$	$C_7H_{19}NO_9PY$
Formula weight	432.32	433.11	436.44	442.55	444.16	449.45	381.11
Crystal system	Monoclinic	Monoclinic	Monoclinic	Monoclinic	Monoclinic	Monoclinic	Monoclinic
Space group	$P2_1/c$	$P2_1/c$	$P2_1/c$	$P2_1/c$	$P2_1/c$	$P2_1/c$	$P2_1/c$
a/Å	5.6906(8)	5.6068(8)	5.5871(6)	5.5462(10)	5.5313(7)	5.5340(10)	5.5234(10)
b/Å	12.8000(18)	13.3820(18)	13.4240(15)	13.343(3)	13.3960(17)	13.436(3)	13.349(2)
c/Å	21.550(3)	21.192(3)	21.157(2)	21.164(4)	20.934(3)	20.891(4)	20.586(4)
β/°	95.392(2)	95.892(2)	96.1480(10)	96.516(3)	96.177(2)	96.159(3)	95.290(2)
V/Å^3	1562.7(4)	1581.6(4)	1577.7(3)	1556.1(5)	1542.2(3)	1544.4(5)	1511.4(5)
Z	4	4	4	4	4	4	4
D_c/g cm^{-3}	1.838	1.819	1.837	1.889	1.913	1.933	1.675
Goodness-of-fit on F^2	1.078	1.087	1.133	1.052	1.079	1.041	1.098
R_1, $[I > 2\sigma(I)]$[b]	0.0643	0.0522	0.0390	0.0626	0.0524	0.0621	0.0710
$wR_2[I > 2\sigma(I)]$[b]	0.1733	0.1414	0.1124	0.1643	0.1337	0.1460	0.2003
R_1, (all data)[b]	0.0982	0.0729	0.0480	0.0988	0.0788	0.1095	0.1025
wR_2 (all data)[b]	0.1954	0.1589	0.1192	0.1871	0.1544	0.1717	0.2247
Largest diff. peak and hole/e Å^{-3}	4.922/−0.905	2.909/−1.155	2.715/−0.761	4.524/−0.874	3.241/−0.951	2.920/−1.255	3.392/−0.677

[a] Including solvent molecules. [b] $R_1 = \Sigma(|F_0| - |F_C|)/\Sigma|F_0|$, $wR_2 = [\Sigma w(|F_0| - |F_C|)^2/\Sigma wF_0^2]^{1/2}$.

(α-Po) net in which each SBU connects six surrounding SBU units through six carboxyphosphonate ligands.

IR spectra

The IR spectra of the eight compounds have many similar features corresponding to the common groups (Fig. S2†), thus only the spectrum of compound **3** will be discussed (Fig. 6). The IR spectrum for compound **3** was recorded in the region 4000–400 cm^{-1}. The broad band around 3365 cm^{-1} corresponds to the O–H stretching vibrations of water molecules. The bands at 1649 cm^{-1}, 1533 cm^{-1} and 1442 cm^{-1} are observed which is shifted from the expected value for an uncoordinated carboxylic acid (ν(C–O) typically around 1725–1700 cm^{-1}). This shift is due to the carboxylate function being coordinated to the metal atom, and these bands are assigned to the asymmetric and symmetric stretching vibrations of C–O groups when present as COO^- moieties.[30] Strong bands between 1200 and 900 cm^{-1} are due to stretching vibrations of the tetrahedral CPO_3 groups, as expected.[31] Additional intense and sharp bands at low energy (769, 665, 607, 511 and 464 cm^{-1} *etc.*) are found, which are probably due to bending vibrations of the tetrahedral CPO_3 groups.

Thermal properties

Thermal gravimetric analyses (TGA) were conducted to examine the stabilities of these compounds. Except for the final weight loss temperature and total weight losses, the TGA curves of compounds **1–8** are very similar, with two main continuous weight losses (Fig. S3†). Herein, we use compound **3** as an example to illuminate the weight losses in detail

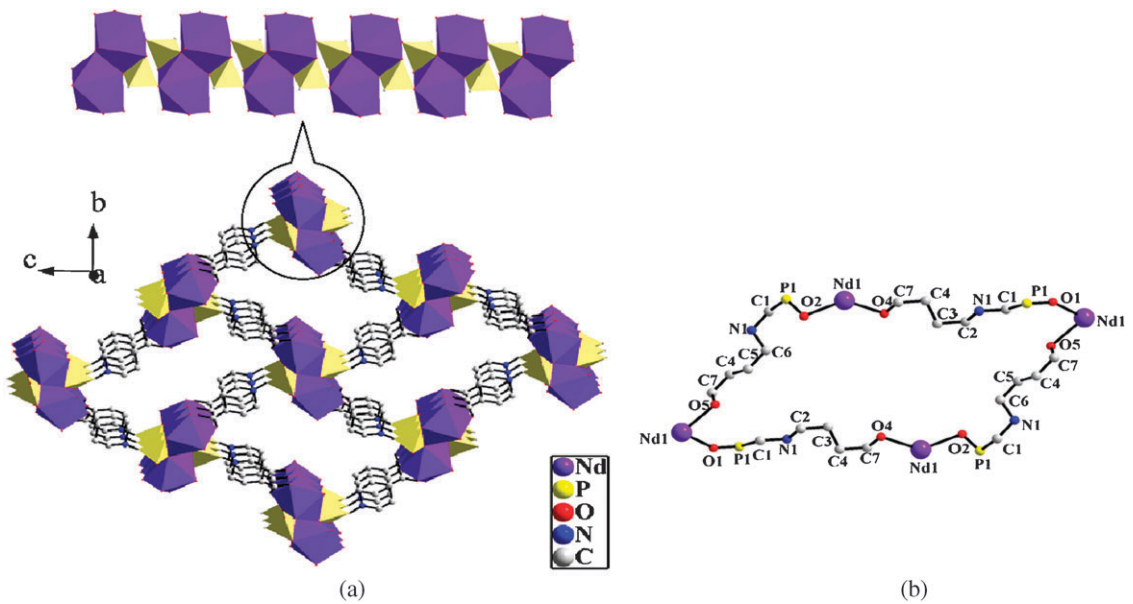

Fig. 3 (a) View of the 3D framework for compound **3** along a-axis showing channels. NdO_8 polyhedra are shaded in purple and CPO_3 tetrahedral are shaded in yellow. (b) The 40-atom rings in compound **3**.

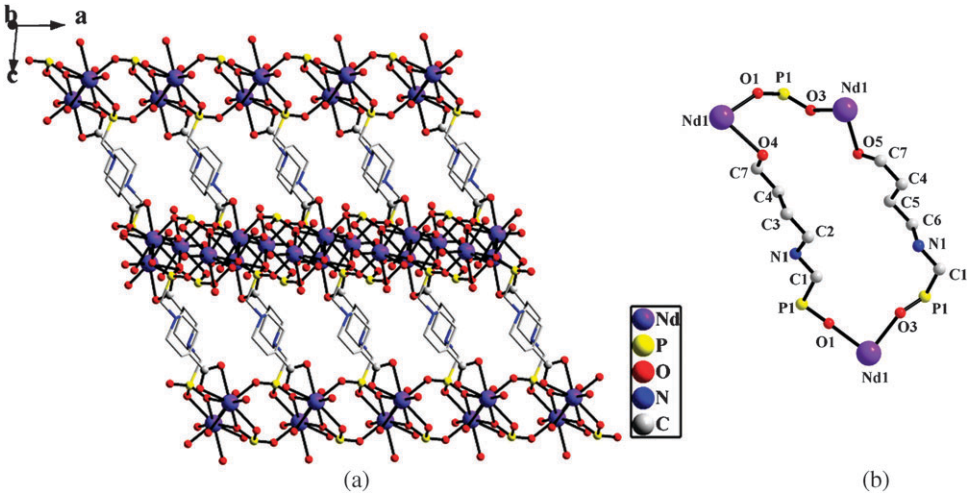

Fig. 4 (a) Ball-and-stick view of the 3D framework for compound **3** along *b*-axis showing the channels. (b) The 24-atom rings in compound **3**.

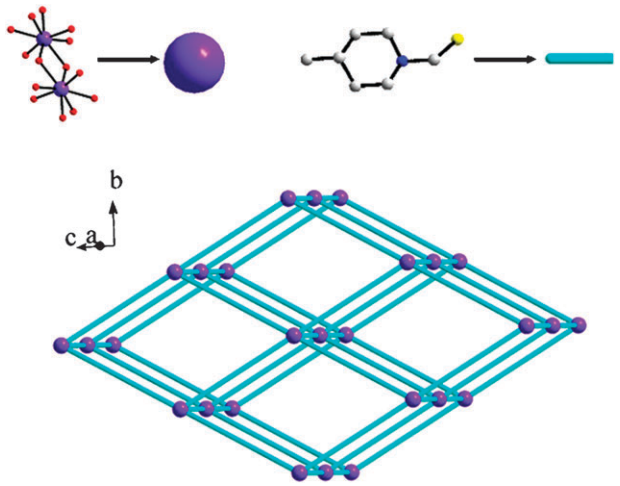

Fig. 5 A simplified representation of compound **3** in which the purple spheres represent the dimer units, and the cyan sticks represent the ligands.

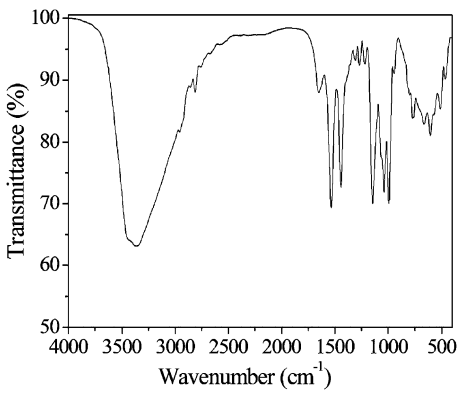

Fig. 6 IR spectrum of compound **3**.

(Fig. 7). The first step started at about 50 °C and was completed at 170 °C, corresponding to the loss of two lattice water molecules and two coordinated water molecules. The observed weight loss of 16.3% is very close to the calculated value (16.5%). The second step, from 340 °C to 700 °C, corresponds to decomposition of the phosphonate group. The final residual of the thermal process is $NdPO_4$ on the basis of powder X-ray diffraction (Fig. S4†). The total weight loss of 45.9% is close to the calculated value (45.2%). The observed total weight losses of compounds **1**, **2** and **4–8** are 47.2%, 47.5%, 45.2%, 45.9%, 44.3%, 52.5% and 44.5%, respectively. The much larger total weight loss for compound **7** (52.5%) is due to its having a much smaller formula weight than the other compounds. During the thermal decomposition, an intermediate compound may be formed between 340 and 650 °C for compound **3**. In order to identify the intermediate compound, X-ray powder diffraction study was performed for compound **3** calcined at 550 °C. However, the intermediate compound was not identified because complicated mixtures were obtained during the thermal decomposition. Considering the thermal stability of these compounds, X-ray powder diffraction studies were performed for the as-synthesized compound **7** and the sample calcined at 200 °C for 2 h under air (Fig. S5†). The XRD patterns for the calcined sample do not fit well with those of the as-synthesized sample, indicating that the structure of these eight compounds is not retained upon dehydration.

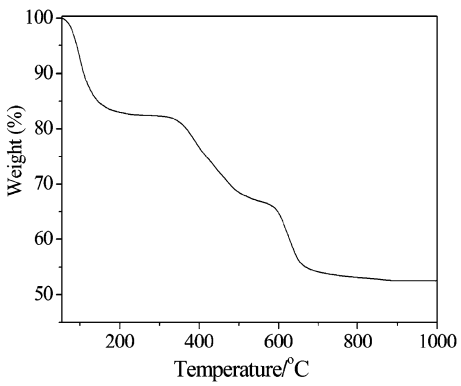

Fig. 7 TGA curve of compound **3**.

Luminescence properties

The solid-state luminescence properties of compounds **5** and **8** were investigated at room temperature. Compound **5** emits red light, which exhibits four sets of characteristic emission bands for the Eu^{3+} ion in the visible region under excitation at 397 nm (Fig. 8). These emission bands arise from $^5D_0 \rightarrow {}^7F_J$ (J = 1, 2, 3, and 4) transitions, in accordance with those typical of the Eu^{3+} ion emission spectrum.[32,33] Two stronger peaks are attributed to $^5D_0 \rightarrow {}^7F_1$ (593 nm) and $^5D_0 \rightarrow {}^7F_2$ (616 nm), and the two weaker peaks belong to the transitions $^5D_0 \rightarrow {}^7F_3$ (650 nm) and $^5D_0 \rightarrow {}^7F_4$ (699 nm). The $^5D_0 \rightarrow {}^7F_1$ transition corresponds to a magnetic dipole transition, and the intensity of this emission for **5** is medium–strong. The most intense emission in the luminescence spectrum is the $^5D_0 \rightarrow {}^7F_2$ transition, which is the so-called hypersensitive transition and is responsible for the brilliant-red emission of compound **5**.[34] It is noted that the intensity of the hypersensitive transition $^5D_0 \rightarrow {}^7F_2$ is comparable to that of $^5D_0 \rightarrow {}^7F_1$. Since the former transition is due to an electric dipole, its intensity is strongly influenced by the crystal field while the latter transition is due to a magnetic dipole and is less sensitive to its environment. The emission spectrum of compound **8** at the excited wavelength 397 nm exhibits the characteristic emission of the Tb^{3+} ion. Characteristic luminescence bands at 488 nm, 543 nm, 589 nm and 622 nm were found (Fig. 9), which correspond to the transitions $^5D_4 \rightarrow {}^7F_6$, $^5D_4 \rightarrow {}^7F_5$, $^5D_4 \rightarrow {}^7F_4$ and $^5D_4 \rightarrow {}^7F_3$, respectively.[28c,33] Of these emission lines, a most striking green luminescence ($^5D_4 \rightarrow {}^7F_5$) for compound **8** is observed in the emission spectrum.

Conclusions

By using the carboxyphosphonic acid as the ligand, eight new lanthanide(III) carboxyphosphonates, $Ln[L(H_2O)_2]\cdot 2H_2O$ (Ln = Ce (**1**), Pr (**2**), Nd (**3**), Sm (**4**), Eu (**5**), Gd (**6**), Y (**7**), Tb (**8**), H_3L = $H_2O_3PCH_2$–NC_5H_9–COOH) have been hydrothermally synthesized and structurally characterized. Compounds **1–8** are isomorphous and feature a 3D framework structure. In these compounds, two LnO_8 polyhedra are interconnected into a dimer through edge-sharing. Each edge-sharing Ln_2O_{14} dimer is linked to another through CPO_3 tetraheda, thereby forming an inorganic chain. Such inorganic chains based on LnO_8 and CPO_3 polyhedra are interconnected through carboxyphosphonate ligands to form a 3D framework structure with a channel system. In addition, compounds **5** and **8**, which exhibit characteristic lanthanide-centered luminescence, are new examples of luminescent rare-earth carboxyphosphonates. Compounds **5** and **8** emit red and green luminescence at room temperature, respectively, and they could be potential fluorescent materials.

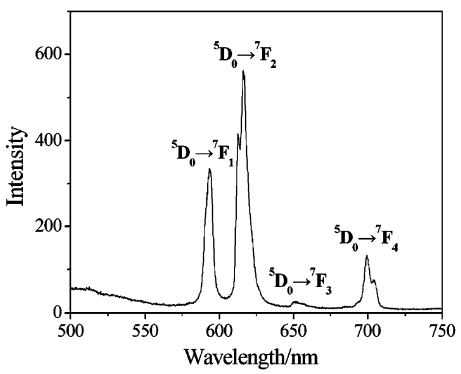

Fig. 8 Solid-state emission spectrum of compound **5** at room temperature.

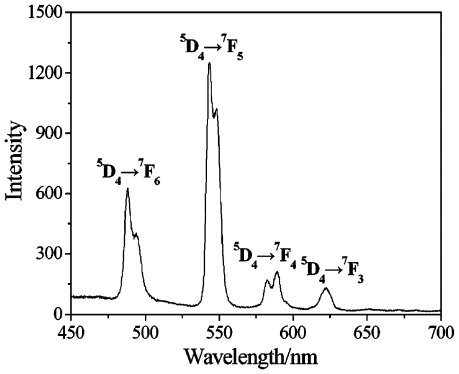

Fig. 9 Solid-state emission spectrum of compound **8** at room temperature.

Experimental

Materials

The carboxyphosphonic acid, $H_2O_3PCH_2$–NC_5H_9–COOH (H_3L), was prepared by a Mannich-type reaction according to the procedures previously described.[35] The lanthanide(III) chlorides were prepared by dissolving corresponding the lanthanide oxides (General Research Institute for Nonferrous Metals, 99.99%) in hydrochloric acid followed by recrystallization and drying. All other chemicals were used as received without further purification.

Physical measurements

Elemental analyses (C, H and N) were performed using a PE-2400 elemental analyzer. Ce, Pr, Nd, Sm, Eu, Gd, Y, Tb and P were determined by using an inductively coupled plasma (ICP) atomic absorption spectrometer. IR spectra were recorded on a Bruker AXS TENSOR-27 FT-IR spectrometer with KBr pellets in the range 4000–400 cm^{-1}. The X-ray powder diffraction data was collected on a Bruker AXS D8 Advance diffractometer using Cu-Kα radiation (λ = 1.5418 Å) in the 2θ range 5–60° with a step size of 0.02° and a scanning rate of 3° min^{-1}. The luminescence spectra were reported on a JASCO FP-6500 spectrofluorimeter (solid). TG analyses were performed on a Perkin–Elmer Pyris Diamond TG-DTA thermal analysis system in static air with a heating rate of 10 K min^{-1} from 50 °C to 1000 °C.

Synthesis

$Ce[L(H_2O)_2]\cdot 2H_2O$ (1). A mixture of $CeCl_3\cdot 6H_2O$ (0.35 g, 1 mmol), H_3L (0.26 g, 1 mmol) and NaOH (0.08 g, 2 mmol) was dissolved in 10.0 mL distilled water. The resulting solution was stirred for about 1 h at room temperature, sealed in a 20 mL Teflon-lined stainless steel autoclave, and then heated at 140 °C for 5 days under autogenous pressure. After the

mixture was cooled slowly to room temperature, colorless blocks were filtered off, washed with distilled water, and dried at room temperature. Yield: 53.8% based on Ce. $C_7H_{19}NO_9PCe$ (432.32): calc. C 19.43, H 4.39, N 3.24, P 7.17, Ce 32.41; found C 19.52, H 4.31, N 3.19, P 7.08, Ce 32.48%. IR (KBr) data: 3373 (s), 1635 (w), 1546 (m), 1431 (m), 1151 (s), 1035 (s), 941 (m), 769 (w), 584 (w), 559 (w), 457 (w) cm^{-1}.

Pr[L(H$_2$O)$_2$]·2H$_2$O (2). The procedure was the same as that for **1** except that $CeCl_3·6H_2O$ was replaced by $PrCl_3·6H_2O$ (0.36 g, 1 mmol). Green blocks of **2** were obtained and washed with water. Yield: 60.1% (based on Pr). $C_7H_{19}NO_9PPr$ (433.11): calc. C 19.39, H 4.39, N 3.23, P 7.16, Pr 32.53; found C 19.31 , H 4.45, N 3.30, P 7.09, Pr 32.48%. IR (KBr) data: 3398 (s), 1629 (w), 1533 (s), 1442 (s), 1143 (s), 1066 (m), 1041 (m), 989 (m), 950 (m), 769 (w), 665 (w), 607 (w), 574 (w), 503 (w), 459 (w) cm^{-1}.

Nd[L(H$_2$O)$_2$]·2H$_2$O (3). The procedure was the same as that for **1** except that $CeCl_3·6H_2O$ was replaced by $NdCl_3·6H_2O$ (0.36 g, 1 mmol). Purple blocks of **3** were obtained and washed with water. Yield: 52.5% (based on Nd). $C_7H_{19}NO_9PNd$ (436.44): calc. C 19.25, H 4.35, N 3.21, P 7.10, Nd 33.05; found C 19.21, H 4.41, N 3.15, P 7.18, Nd 33.12%. IR (KBr) data: 3365 (s), 1649 (w), 1533 (m), 1442 (m), 1143 (m), 1041 (m), 995 (m), 769 (w), 665 (w), 607 (w), 511 (w), 464 (w) cm^{-1}.

Sm[L(H$_2$O)$_2$]·2H$_2$O (4). The procedure was the same as that for **1** except that $CeCl_3·6H_2O$ was replaced by $SmCl_3·6H_2O$ (0.37 g, 1 mmol). Pale yellow blocks of **4** were obtained and washed with water. Yield: 43.6% (based on Sm). $C_7H_{19}NO_9PSm$ (442.55): calc. C 18.98, H 4.29, N 3.16, P 7.00, Sm 33.98; found C 18.89, H 4.35, N 3.12, P 7.08, Sm 33.91%. IR (KBr) data: 3442 (s), 1654 (w), 1533 (m), 1450 (m), 1311 (w), 1265 (w), 1220 (w), 1137 (m), 1029 (m), 991 (m), 954 (m), 813 (w), 788 (w), 761 (w), 667 (w), 603 (w), 507 (w), 462 (w) cm^{-1}.

Eu[L(H$_2$O)$_2$]·2H$_2$O (5). A mixture of H_3L (0.07 g, 0.25 mmol), $EuCl_3·6H_2O$ (0.10 g, 0.25 mmol) and NaOH (0.04 g, 1 mmol) in 12 mL deionized water. The resulting solution was stirred for about 1 h at room temperature, sealed in a 20 ml Teflon-lined stainless steel autoclave, and then heated at 120 °C for 5 days. Colorless blocks of **5** were obtained and washed with water. Yield: 45.7% based on Eu. $C_7H_{19}NO_9PEu$ (444.16): calc. C 18.91, H 4.28, N 3.15, P 6.98, Eu 34.21; found C 18.85, H 4.35, N 3.19, P 6.92, Eu 34.28%. IR (KBr) data: 3450 (s), 1649 (w), 1533 (m), 1442 (m), 1313 (w), 1272 (w), 1217 (w), 1137 (m), 995 (m), 761 (w), 671 (w), 613 (w), 511 (w), 464 (w) cm^{-1}.

Gd[L(H$_2$O)$_2$]·2H$_2$O (6). A mixture of H_3L (0.13 g, 0.5 mmol), $GdCl_3·6H_2O$ (0.19 g, 0.5 mmol) and NaOH (0.04 g, 1 mmol) in 10 mL deionized water. The resulting solution was stirred for about 1 h at room temperature, sealed in a 20 ml Teflon-lined stainless steel autoclave, and then heated at 140 °C for 5 days. Colorless blocks of **6** were obtained and washed with water. Yield: 57.4% based on Gd. $C_7H_{19}NO_9PGd$ (449.45): calc. C 18.69, H 4.23, N 3.11, P 6.90, Gd 34.99; found C 18.61, H 4.28, N 3.05, P 6.97, Gd 34.92%. IR (KBr) data: 3431 (s), 1647 (w), 1533 (m), 1450 (m), 1303 (w), 1271 (w), 1220 (w), 1145 (m), 1074 (w), 1035 (m), 990 (m), 960 (w), 813 (w), 788 (w), 769 (w), 667 (w), 603 (w), 507 (w), 457 (w) cm^{-1}.

Y[L(H$_2$O)$_2$]·2H$_2$O (7). The procedure was the same as that for **1** except that $CeCl_3·6H_2O$ was replaced by $YCl_3·6H_2O$ (0.30 g, 1 mmol). Colorless blocks of **7** were obtained and washed with water. Yield: 55.6% (based on Y). $C_7H_{19}NO_9PY$ (381.11): calc. C 22.04, H 4.99, N 3.67, P 8.13, Y 23.33; found C 22.11, H 4.93, N 3.74, P 8.09, Y 23.38%. IR (KBr) data: 3423–3207 (s, br), 1629 (w), 1546 (m), 1450 (m), 1303 (w), 1265 (w), 1215 (w), 1157 (s), 1118 (m), 1074 (m), 1043 (m), 1010 (m), 941 (w), 819 (w), 769 (w), 655 (w), 609 (w), 507 (w), 462 (w) cm^{-1}.

Tb[L(H$_2$O)$_2$]·2H$_2$O (8). A mixture of H_3L (0.26 g, 1 mmol), $TbCl_3·6H_2O$ (0.37 g, 1 mmol) and NaOH (0.10 g, 2.5 mmol) in 10 mL deionized water. The resulting solution was stirred for about 1 h at room temperature, sealed in a 20 ml Teflon-lined stainless steel autoclave, and then heated at 80 °C for 4 days. The colorless powder of **8** was obtained and washed with water. Yield: 49.7% based on Tb. $C_7H_{19}NO_9PTb$ (451.13): calc. C 18.62, H 4.21, N 3.10, P 6.87, Tb 35.23; found C 18.68, H 4.15, N 3.18, P 6.81, Tb 35.15%. IR (KBr) data: 3436 (m), 1654 (w), 1539 (m), 1450 (m), 1305 (w), 1267 (w), 1222 (w), 1143 (m), 1041 (m), 1002 (m), 775 (w), 671 (w), 613 (w), 516 (w), 464 (w) cm^{-1}.

Crystallographic determinations

Data collections for compounds **1–7** were performed on a Bruker Smart APEX II X-diffractometer equipped with graphite-monochromated Mo-Kα radiation (λ = 0.71073 Å) at 293 ± 2 K. An empirical absorption correction was applied using the SADABS program. All structures were solved by direct methods and refined by full-matrix least squares fitting on F^2 by SHELXS-97.[36] All non-hydrogen atoms were refined anisotropically. All hydrogen atoms were placed in geometrically idealized positions and constrained to ride on their parent atoms. In the structure of compounds **1**, **2**, **3** and **7**, the oxygen atoms of lattice water molecules are disordered, the same as the several carbon atoms in compounds **4** and **6**. Multiple structural restraints were applied for these atoms in the refinement. The oxygen atoms of lattice water molecules are disordered, so the large electron density peaks remaining are in close proximity to the oxygen atoms of lattice water molecules.

Acknowledgements

This research was supported by grants from the Education Department of Liaoning Province of China (2009S063).

References

1 (*a*) K. Maeda, *Microporous Mesoporous Mater.*, 2004, **73**, 47and references therein; (*b*) J.-D. Wang, A. Clearfield and G.-Z. Peng, *Mater. Chem. Phys.*, 1993, **35**, 208; (*c*) C. Y. Ortiz-Avila, C. Bhardwaj and A. Clearfield, *Inorg. Chem.*, 1994, **33**, 2499.
2 (*a*) A. Clearfield, *Curr. Opin. Solid State Mater. Sci.*, 1996, **1**, 268; (*b*) G. E. Fanucci, J. Krzystek, M. W. Meisel, L. C. Brunel and D. R. Talham, *J. Am. Chem. Soc.*, 1998, **120**, 5469.

3 G. Alberti and U. Costantino, in *Comprehensive Supramolecular Chemistry*, ed. J. M. Lehn, Pergamon-Elsevier Science Ltd, London, 1996, p. 1.
4 (*a*) A. Clearfield, *Progress in Inorganic Chemistry*, 1998, vol. 47, p. 371; (*b*) T. Kimura, *Chem. Mater*., 2003, **15**, 3742.
5 (*a*) T. E. Mallouk and J. A. Gavin, *Acc. Chem. Res*., 1998, **31**, 209; (*b*) F. Odobel, B. Bujoli and D. Massiot, *Chem. Mater*., 2001, **13**, 163; (*c*) K. Maeda, Y. Kiyozumi and F. Mizukami, *J. Phys. Chem. B*, 1997, **101**, 4402.
6 O. R. Evans, H. L. Ngo and W.-B. Lin, *J. Am. Chem. Soc*., 2001, **123**, 10395.
7 J. A. Groves, P. A. Wright and P. Lightfoot, *Dalton Trans*., 2005, 2007.
8 J. A. Groves, S. R. Miller, S. J. Warrender, C. M. Draznieks, P. Lightfoot and P. A. Wright, *Chem. Commun*., 2006, 3305.
9 G. B. Hix, A. Turner, L. Vahter and B. M. Kariuki, *Microporous Mesoporous Mater*., 2007, **99**, 62.
10 Z.-Y. Du, A. V. Prosvirin and J.-G. Mao, *Inorg. Chem*., 2007, **46**, 9884.
11 Y.-Q. Guo, B.-P. Yang, J.-L. Song and J.-G. Mao, *Cryst. Growth Des*., 2008, **8**, 600.
12 P. Yin, S. Gao, L.-M. Zheng and X.-Q. Xin, *Chem. Mater*., 2003, **15**, 3233.
13 J.-L. Song and J.-G. Mao, *J. Solid State Chem*., 2005, **178**, 3514.
14 (*a*) N. Stock and T. Bein, *J. Mater. Chem*., 2005, **15**, 1384; (*b*) K. D. Demadis, P. Lykoudis, R. G. Raptis and G. Mezei, *Cryst. Growth Des*., 2006, **6**, 1064.
15 D. Kong and A. Clearfield, *Cryst. Growth Des*., 2005, **5**, 1263.
16 B.-P. Yang, A. V. Prosvirin, Y.-Q. Guo and J.-G. Mao, *Inorg. Chem*., 2008, **47**, 1453.
17 (*a*) A. K. Cheetham, G. Ferey and T. Loiseau, *Angew. Chem., Int. Ed*., 1999, **38**, 3268; (*b*) J. Zhu, X. Bu, P. Feng and G. D. Stucky, *J. Am. Chem. Soc*., 2000, **122**, 11563.
18 (*a*) S. Drumel, P. Janvier, P. Barboux, M. Bujoli-Doeuff and B. Bujoli, *Inorg. Chem*., 1995, **34**, 148; (*b*) F. Fredoueil, M. Evain, D. Massiot, M. Bujoli-Doeuff, P. Janvier, A. Clearfield and B. Bujoli, *J. Chem. Soc., Dalton Trans*., 2002, 1508; (*c*) P. Rabu, P. Janvier and B. Bujoli, *J. Mater. Chem*., 1999, **9**, 1323.
19 (*a*) A. Distler and S. C. Sevov, *Chem. Commun*., 1998, 959; (*b*) N. Stock, S. A. Frey, G. D. Stucky and A. K. Cheetham, *J. Chem. Soc., Dalton Trans*., 2000, 4292; (*c*) S. Ayyappan, G. D. de Delgado, A. K. Cheetham, G. Ferey and C. N. R. Rao, *J. Chem. Soc., Dalton Trans*., 1999, 2905.
20 S.-F. Tang, J.-L. Song and J.-G. Mao, *Eur. J. Inorg. Chem*., 2006, 2011.
21 J.-L. Song and J.-G. Mao, *Chem. Eur. J*., 2005, **11**, 1417.
22 Q. Yue, J. Yang, G.-H. Li, G.-D. Li and J.-S. Chen, *Inorg. Chem*., 2006, **45**, 4431.
23 C. Serre, N. Stock, T. Bein and G. Férey, *Inorg. Chem*., 2004, **43**, 3159.
24 J. Zhang, J. Li, Z.-G. Sun, R.-N. Hua, Y.-Y. Zhu, Y. Zhao, N. Zhang, L. Liu, X. Lu, W.-N. Wang and F. Tong, *Inorg. Chem. Commun*., 2009, **12**, 279.
25 (*a*) Y.-Y. Zhu, Z.-G. Sun, H. Chen, J. Zhang, Y. Zhao, N. Zhang, L. Liu, X. Lu, W.-N. W and F. Tong, *Cryst. Growth Des*., 2009, **9**, 3288; (*b*) Y.-Y. Zhu, Z.-G. Sun, Y. Zhao, J. Zhang, X. Lu, N. Zhang, L. Liu and F. Tong, *New J. Chem*., 2009, **33**, 119; (*c*) Y. Zhao, J. Li, Z.-G. Sun, J. Zhang, Y.-Y. Zhu, X. Lu, L. Liu and N. Zhang, *Inorg. Chem. Commun*., 2008, **11**, 1057.
26 (*a*) J. A. Groves, P. A. Wright and P. Lightfoot, *Inorg. Chem*., 2005, **44**, 1736; (*b*) J. A. Groves, N. F. Stephens, P. A. Wright and P. Lightfoot, *Solid State Sci*., 2006, **8**, 397.
27 J. P. Silvestre, N.-Q. Dao and M. R. Lee, *Phosphorus, Sulfur Silicon Relat. Elem*., 2001, **176**, 173.
28 (*a*) J. Legendziewicz, P. Gawryszewska, E. Gałdecka and Z. Gałdecki, *J. Alloys Compd*., 1998, **275**, 356; (*b*) F. Serpaggi and G. Férey, *Inorg. Chem*., 1999, **38**, 4741; (*c*) S.-F. Tang, J.-L. Song, X.-L. Li and J.-G. Mao, *Cryst. Growth Des*., 2006, **6**, 2322.
29 S.-M. Ying and J.-G. Mao, *Cryst. Growth Des*., 2006, **6**, 964.
30 (*a*) G. B. Hix, D. S. Wragg, P. A. Wright and R. E. Morris, *J. Chem. Soc., Dalton Trans*., 1998, 3359; (*b*) A. Cabeza, M. A. G. Aranda and S. Bruque, *J. Mater. Chem*., 1998, **8**, 2479.
31 (*a*) A. Cabeza, X. Ouyang, C. V. K. Sharma, M. A. G. Aranda, S. Bruque and A. Clearfield, *Inorg. Chem*., 2002, **41**, 2325; (*b*) Z.-M. Sun, J.-G. Mao, B.-P. Yang and S.-M. Ying, *Solid State Sci*., 2004, **6**, 295.
32 J.-G. Mao, *Coord. Chem. Rev*., 2007, **251**, 1493.
33 S.-S. Bao, L.-F. Ma, Y. Wang, L. Fang, C.-J. Zhu, Y.-Z. Li and L.-M. Zheng, *Chem. Eur. J*., 2007, **13**, 2333.
34 (*a*) A. de Bettencourt-Dias, *Inorg. Chem*., 2005, **44**, 2737; (*b*) G. L. Law, K. L. Wong, X. Zhou, W. T. Wong and P. A. Tanner, *Inorg. Chem*., 2005, **44**, 4142.
35 K. Moedritzer and R. R. Irani, *J. Org. Chem*., 1966, **31**, 1603.
36 G. M. Sheldrick, *SHELXS–97, Program for X-ray Crystal Structure Solution and Refinement*, University of Göttingen, Germany, 1997.